A self-consistent solution of Schrödinger–Poisson equations using a nonuniform mesh

I-H. Tan, G. L. Snider, L. D. Chang, and E. L. Hu

Articles you may be interested in

A self-consistent solution of Schrödinger–Poisson equations using a nonuniform mesh

I-H. Tan, G. L. Snider, L. D. Chang, and E. L. Hu

Department of Electrical and Computer Engineering, University of California, Santa Barbara, California 93106

A self-consistent, one-dimensional solution of the Schrödinger and Poisson equations is obtained using the finite-difference method with a nonuniform mesh size. The use of the proper matrix transformation allows preservation of the symmetry of the discretized Schrödinger equation, even with the use of a nonuniform mesh size, therefore reducing the computation time. This method is very efficient in finding eigenstates extending over relatively large spatial areas without loss of accuracy. For confirmation of the accuracy of this method, a comparison is made with the exactly calculated eigenstates of GaAs/AlGaAs rectangular wells. An example of the solution of the conduction band and the electron density distribution of a single-heterostructure GaAs/AlGaAs is also presented.

I. INTRODUCTION

Growth of high-quality heterostructure wells, together with lateral feature modulation either by high-resolution fabrication processes[1,2] or, more recently, by innovative growth on tilted substrates[3,4] are producing structures and devices of low dimensionality whose device implications may be far reaching. Full understanding of the optical and transport properties of these structures requires the self-consistent solution of both Poisson and Schrödinger equations.[5-8]

A conventional approach to the solution of the Schrödinger equation has been the finite-difference method (FDM). Real space is divided into discrete mesh points and the wave function is solved within those discrete spacings. Solving the differential equation within each mesh spacing results in a vector solution for ψ, and a matrix formulation of the Schrödinger equation:

$$A\psi = \lambda\psi, \tag{1}$$

where A is the matrix operator and λ the energy eigenvalues. The implementation of FDM usually makes use of uniform mesh spacings so that A is real and symmetric. The mesh size is determined by the opposing requirements of greater accuracy on one hand (hence, smaller mesh size) and rapid computation times on the other hand (hence large mesh size).

However, there are many cases where the wave function rapidly varies within one region, and then changes slowly over another region. For example, Fig. 1(a) shows the wave function at the GaAs/AlGaAs single heterojunction, with an energy eigenvalue close to the Fermi level. In such a case, the ideal situation would be to use a variable mesh size: smaller mesh in region I, and large spacing in region II. The use of a variable mesh, however, requires careful treatment at the juncture of two different mesh sizes and destroys the symmetry of the matrix A, in turn making the eigenfunction more difficult to compute.[9] In this paper, we propose a simple matrix transformation that will preserve the symmetry of the matrix while allowing variable mesh size. If the optimal nonuniform mesh is used, this method will provide a compu-

tationally efficient solution of the band profile and the electron density distributed over a large spatial dimension.

The equations used and the iterative procedure for obtaining self-consistent Schrödinger and Poisson solutions is described in Sec. II. Section III describes the matrix transformation used to preserve the symmetry of the discretized Schrödinger equation and the Newton method to solve the Poisson equation. A heterojunction quantum well and the single heterostructure with modulated doping are given as exemplary solutions in Sec. IV. Finally, the paper is summarized in Sec. V.

II. BASIC EQUATIONS

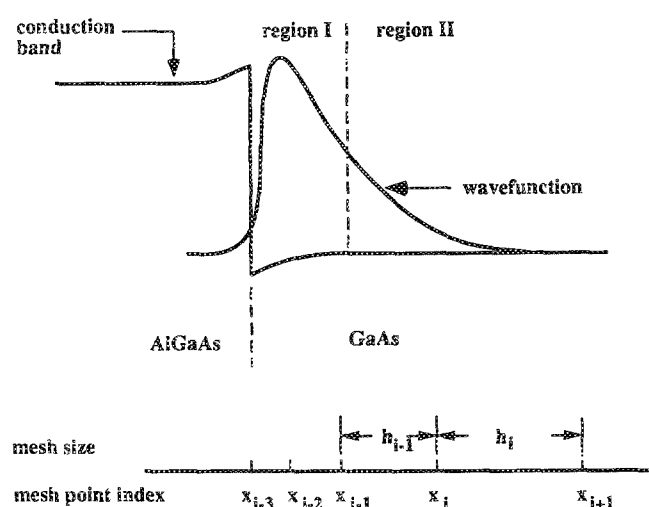The one-dimensional, one-electron Schrödinger equation is

FIG. 1.(a) Band diagram of the single-heterojunction GaAs/AlGaAs and its bounded state wave functions. (b) Discretization of the potential using a nonuniform mesh.

$$-\frac{\hbar^2}{2}\frac{d}{dx}\left(\frac{1}{m^*(x)}\frac{d}{dx}\right)\psi(x) + V(x)\psi(x) = E\psi(x), \quad (2)$$

where ψ is the wave function, E is the energy, V is the potential energy, $\hbar$ is Planck's constant divided by 2π, and m^* is the effective mass. The one-dimensional Poisson equation is

$$\frac{d}{dx}\left(\epsilon_s(x)\frac{d}{dx}\right)\phi(x) = \frac{-q[N_D(x) - n(x)]}{\epsilon_0}, \quad (3)$$

where ϵ_s is the dielectric constant, ϕ is the electrostatic potential, N_D is the ionized donor concentration, and n is the electron density distribution. To find the electron distribution in the conduction band, one may set the potential energy V to be equal to the conduction-band energy. In a quantum well of arbitrary potential energy profile, the potential energy V is related to the electrostatic potential ϕ as follows:

$$V(x) = -q\phi(x) + \Delta E_c(x), \quad (4)$$

where ΔE_c is the pseudopotential energy due to the band offset at the heterointerface. The wave function $\psi(x)$ in Eq. (2) and the electron density $n(x)$ in Eq. (3) are related by

$$n(x) = \sum_{k=1}^{m}\psi_k^*(x)\psi_k(x)n_k, \quad (5)$$

where m is the number of bound states, and n_k is the electron occupation for each state. The electron concentration for each state can be expressed by

$$n_k = \frac{m^*}{\pi\hbar^2}\int_{E_k}^{\infty}\frac{1}{1 + e^{(E-E_F)/kT}}dE, \quad (6)$$

where E_k is the eigenenergy.

We use an iteration procedure to obtain self-consistent solutions for Eqs. (2) and (3). Starting with a trial potential $V(x)$, the wave functions, and their corresponding eigenenergies, E_k can be used to calculate the electron density distribution $n(x)$ using Eqs. (5) and (6). The computed $n(x)$ and a given donor concentration $N_D(x)$ can be used to calculate $\phi(x)$ via Eq. (3). The new potential energy $V(x)$ is then obtained from Eq. (4). The subsequent iteration will yield the final self-consistent solutions for $V(x)$ and $n(x)$ which satisfy certain error criteria.

III. NUMERICAL METHOD

A. Formulation for the Schrödinger equation

In order to numerically solve the Schrödinger equation, we may discretize the differential equation (3) by using a three-point finite difference scheme as shown in Fig. 1(b):

$$-\frac{\hbar^2}{2}\left(\frac{2(\psi_{i+1} - \psi_i)}{m_{i+1/2}h_i(h_i + h_{i-1})}\right.$$
$$\left. - \frac{2(\psi_i - \psi_{i-1})}{m_{i-1/2}h_{i-1}(h_i + h_{i-1})}\right) = \lambda\psi_i.$$

This may be cast in the form of a matrix equation,

$$\sum_{j=1}^{n}A_{ij}\psi_j = \lambda\psi_i, \quad (7)$$

where

$$A_{ij} = \begin{cases} -\dfrac{\hbar^2}{2}\left(\dfrac{2}{m^*_{i+1/2}}\dfrac{1}{h_{i+1}(h_i + h_{i-1})}\right) & \text{if } j = i+1, \\[2ex] -\dfrac{\hbar^2}{2}\left(\dfrac{2}{m^*_{i-1/2}}\dfrac{1}{h_{i+1}(h_i + h_{i-1})}\right) & \text{if } j = i-1, \\[2ex] -A_{ii+1} - A_{ii-1} + V_i & \text{if } j = i, \\[1ex] 0 & \text{otherwise.} \end{cases} \quad (8)$$

The index i identifies the grid point on the one-dimensional mesh. Half-integer index implies a point midway between the grid points, and h_i is the mesh size between adjacent grid points x_i and x_{i+1}. This gives a tridiagonal matrix which appears symmetric only if the mesh spacings h_i are all uniform. While the use of a nonuniform mesh size might be preferable for certain problems, this would destroy the symmetry of the matrix A and hence obviate computational simplifications that result from the symmetry. However, if we define the following parameter:

$$L_i^2 = (h_i + h_{i-1})/2, \quad (9)$$

Eq. (8) becomes

$$A_{ij} = \begin{cases} -\dfrac{\hbar^2}{2}\left(\dfrac{1}{m^*_{i+1/2}}\dfrac{1}{h_i}\right)\dfrac{1}{L_i^2} & \text{if } j = i+1, \\[2ex] -\dfrac{\hbar^2}{2}\left(\dfrac{1}{m^*_{i-1/2}}\dfrac{1}{h_{i-1}}\right)\dfrac{1}{L_i^2} & \text{if } j = i-1, \\[2ex] -A_{ii+1} - A_{ii-1} + V_i & \text{if } j = i, \\[1ex] 0 & \text{otherwise.} \end{cases} \quad (8')$$

We set $B_{ij} = L_i^2 A_{ij}$, or in matrix notation,

$$B = MA, \quad (10)$$

where M is the diagonal matrix whose elements are L_i^2. As the product of a diagonal and triadiagonal matix, B is tridiagonal. From Eqs. (9) and (8'), it is easily seen that B is symmetric, i.e., $B_{ii+1} = B_{i+1i}$. This provides the desired transformation that allows us to solve for

$$B\Psi = MA\psi = \lambda M\Psi. \quad (11)$$

The matrix M obtained from the FDM method is diagonal so that we may easily express it in the form

$$M = LL, \quad (12)$$

where L is a diagonal matrix whose elements are L_i.

Using (10), we can show that

$$L^{-1}BL^{-1}L\psi = L^{-1}LLA\psi = \lambda L^{-1}LL\psi,$$

or

$$H\Phi = \lambda\Phi, \quad (13)$$

where

$$H = L^{-1}BL^{-1} \quad (14)$$

and

$$\psi = L^{-1}\Phi. \quad (15)$$

Since the relation $H = H^T$ holds because B is symmetric and L is diagonal, the matrix H is a symmetric and tridiagonal matrix. Equation (13) is now the central equation for finding the eigenvalues and eigenfunctions. Therefore, instead of

solving Eq. (1), one may solve Eq. (13) to obtain the eigenvalue λ corresponding to the eigenfunction Φ. Then one may use Eq. (15) to obtain the wave function ψ from Φ. If ψ_k and ψ_l are two wave functions in the potential well, they are related to each other by

$$\psi_k^T M \psi_l = \begin{cases} 1 & \text{if } k = l, \\ 0 & \text{if } k \neq l, \end{cases} \quad (16)$$

which means those wave functions are orthonormal to one another with respect to the weighting matrix M.

It is noted that this method can be applied not only in one-dimensional cases but also in two-dimensional ones. Using the same approach to discretize the two-dimensional Schrödinger equation, we may obtain the same equation as (11) in which B turns out to be banded and symmetric and M is still diagonal. Therefore, after the same matrix transformation, we may obtain Eq. (13).

B. Formulation for Poisson's equation

Newton's method is used in solving the nonlinear Poisson's equation (see the Appendix). The differential equation describing the incremental potential change $\delta\phi$ at each iteration satisfies the equation

$$-\left[\frac{d}{dx}\left(\epsilon_s \frac{d\phi}{dx}\right) + \frac{q}{\epsilon_0}\left[N_D(x) - n(x)\right]\right]$$

$$= \frac{d}{dx}\left(\epsilon_s \frac{d\delta\phi}{dx}\right) + \frac{q}{\epsilon_0}\sum_{k=1}^{m} \psi_k^* \psi_k \frac{\partial n_k}{\partial E_k}\langle\psi_k|q\delta\phi|\psi_k\rangle. \quad (17)$$

In the equation above, we have assumed that the donors are completely ionized and the variation of wave function versus $\delta\phi$ is very small. The term on the left-hand side of the above equation is the error and it is zero if the electrostatic potential ϕ is equal to the self-consistent solution. Although this differential-integral equation is hard to solve, a first-order approximation can be made by setting the integral result of the bra-ket to be $q\delta\phi$.[10] From Eq. (6) we may also calculate the partial derivative, $\partial n_k/\partial E_k$. Therefore, using the same method to discretize the Poisson equation as that used for the Schrödinger equation, Eq. (17) can be expressed as

$$-e_i = C_{ii+1}\delta\phi_{i+1}$$

$$+ \delta\phi_i\left(C_{ii} + \frac{q}{\epsilon_0}\sum_{\kappa=1}^{m} \psi_{\kappa i}^* \psi_{\kappa i}\right.$$

$$\left.\times\frac{qm^*}{\pi\hbar^2(1 + e^{(E_k - E_F)/kT})}\right) + C_{ii-1}\delta\phi_{i-1}, \quad (18)$$

where

$$e_i = \sum_{j=1}^{n} C_{ij}\phi_j + q(N_{Di} - n_i)/\epsilon_0, \quad (19)$$

$$C_{ij} = \begin{cases} \dfrac{2\epsilon_{i+1/2}}{h_i(h_i + h_{i-1})} & \text{if } j = i + 1, \\[3mm] \dfrac{2\epsilon_{i+1/2}}{h_i(h_i + h_{i-1})} & \text{if } j = i - 1, \\[3mm] -C_{ii+1} - C_{ii-1} & \text{if } i = j, \\[1mm] 0 & \text{otherwise.} \end{cases} \quad (20)$$

Thus, in Eq. (18) there are n error equations with n un-

known variables $(\delta\phi_1, \delta\phi_2, ..., \delta\phi_n)$. They may be manipulated as a matrix equation:

$$C'\delta\phi = -\xi, \quad (21)$$

where C' is a tridiagonal, nonsymmetric, and $n \times n$ matrix, $\delta\phi$ is the $n \times 1$ vector containing the corrected potential at each point which must be added to the former potential profiles, and ξ is a $n \times 1$ vector including the Poisson error at each point. Now, Eq. (21) is the central equation required to modify the former potential profile. To maximize the computing efficiency and to save the memory space, Crout's reduction method[11] is used for solving Eq. (21) where the matrix C' is tridiagonal.

IV. RESULTS

A. Rectangular quantum well

To evaluate the validity and the accuracy of the present method using the nonuniform mesh, we first consider the eigenstates of an electron in a simple rectangular quantum well of GaAs/Al$_{0.3}$Ga$_{0.7}$As, as shown in Fig. 2(a). The width of the well is chosen to be 56 Å so that the upper (of two) bound energy eigenvalues is very close to the height of the potential barrier, so that the corresponding wave function extends over a large distance outside the well. We consider the conduction band only so that the exact solutions

(a)

(b)
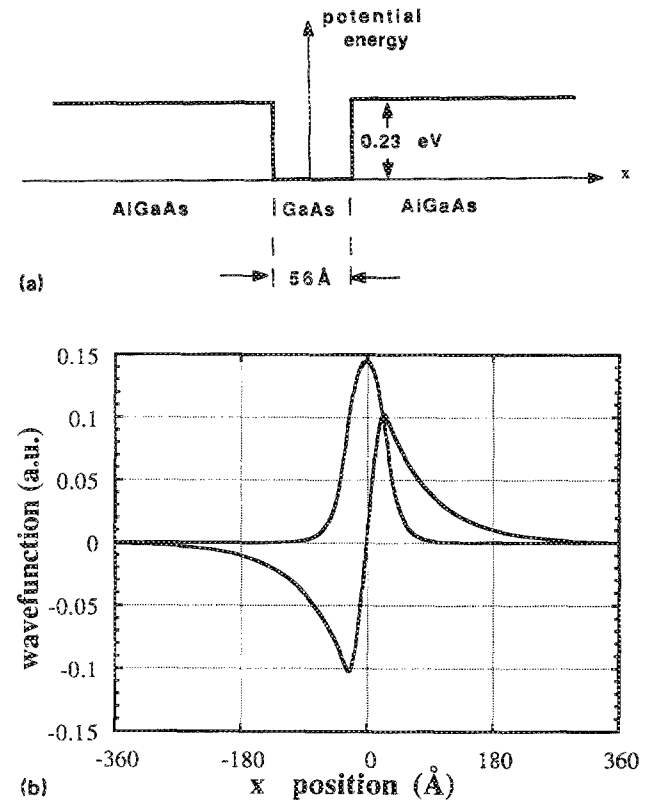
FIG. 2.(a) Rectangular quantum well of GaAs/AlGaAs:m^*(GaAs) $= 0.067m_0$, m^*(AlGaAs) $= 0.092m_0$, $\Delta E_c = 0.23$ eV. The variable mesh size is chosen in different regions, ranging from 2 Å inside the well to 32 Å far away from the well. (b) The bound eigenfunctions for the rectangular quantum well.

n	Exact solution (meV)	Uniform mesh (4 Å)		Uniform mesh (8 Å)		Nonuniform mesh (2–32 Å)	
		No. of meshes	FDM solution/error (meV/%)	No. of meshes	FDM solution/error (meV/%)	No. of meshes	FDM solution/error (meV/%)
1	64.24722	194	63.81747/0.669	97	62.56356/2.621	104	64.28038/0.052
2	220.7776	194	220.3347/0.201	97	218.9136/0.844	104	220.6846/0.042

can be obtained by solving the transcendental equations and we can check the validity of our method. The transcendental equations can be obtained from the connection rules (the wave function and its derivative divided by the effective mass continuous at the heterojunction of GaAs/AlGaAs. The two bound wave functions are depicted in Fig. 2(b). The width of the total region of interest is 768 Å, 13 times larger than that of the quantum well, to ensure the validity of the boundary conditions.

Calculations using a nonuniform mesh (size ranging from 2 to 32 Å) have been made for the same potential. The more standard computation, using a uniform mesh of 4 or 8 Å size, was also carried out. Table I shows the calculated eigenenergies of the quantum well, using both uniform mesh and nonuniform mesh. The corresponding errors of the eigenenergies, compared with the exact solutions are also listed. We observe that the percent error becomes smaller as the the mesh size is reduced. The number of grids in the case of nonuniform mesh is close to that in the case of uniform mesh with 8 Å size while the percent error of the former case is much smaller than the latter one. We also notice that, in all cases, the percent error for the second bound state is smaller than that for the first bound state. This is because the second bound state changes far less rapidly than the ground state, as shown in Fig. 4.

B. Single-heterojunction GaAs/AlGaAs

Now, consider a modulation-doped GaAs/Al$_{0.3}$Ga$_{0.7}$As structure as shown in Fig. 3. In this case, the electrons are weakly confined at the quasi-one-dimensional heterojunction. The wave functions rapidly vary within the kink of the conduction band, and then change slowly over a long distance because of the smooth and slow change of potential barrier.
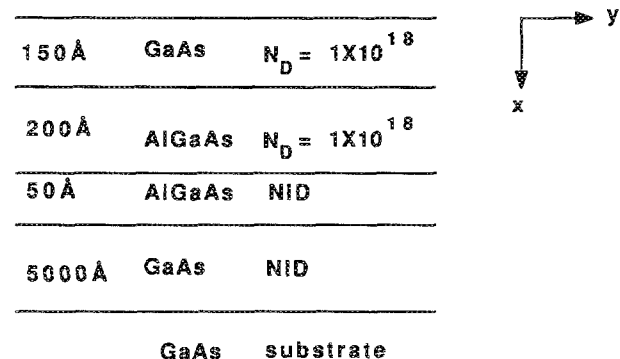
A nonuniform mesh, ranging from 2 Å at the vicinity of the heterointerface to 32 Å when the mesh is far away from the heterointerface, is used in implementing this method. To solve Poisson's equation, the boundary conditions imposed on the structure are that the conduction band must equal the barrier height at the surface, and the normal derivative must be zero at the substrate. Likewise, the Neumann-type boundary conditions have been assumed for the Schrödinger equation. Since only bound states are considered, both the wave function and its derivative should go to zero at the boundary. If the wave function at the edge of the mesh is not close to zero, the state is not a valid bound state. These boundary conditions allow a quick check of the validity of

both wave functions and conduction band. For convenience, the Fermi level in the conduction band has been chosen to be the reference zero point. The temperature is assumed to be 4 K. To fulfill the requirements of the boundary conditions, the width of the region is 4500 Å large and the number of mesh points is 450. The convergence criterion is that the minimum of $\delta\phi_i$ should be smaller than 10^{-5} V at the last run of iteration. After the convergence criterion is satisfied, a final check of the validity of the approximation using Newton's method is made by comparing the ratio of the right-hand term to the left-hand term in Eq. (3). In general, the difference between this ratio and 1 is smaller than 0.002 at all mesh points, indicating that the approximation using Newton's method is a good one. Once the solution for the discretized Poisson's equation has been found, it should be the unique and self-consistent solution for both equations.[12]

There are two bound states in this case. After iterating between the Schrödinger equation and the Poisson equation, the convergent solutions of both conduction band and electron density distribution are shown in Fig. 4. We observe that the distance between the position of the peak electron density and the heterointerface is 85 Å. The tail of the electron density distribution for $x > 800$ Å primarily results from the electrons occupying the second bound state.

V. CONCLUSION

In this paper, we present a finite-difference method to self-consistently solve the Schrödinger equation and the Poisson equation. We use a simple matrix transformation

150 Å	GaAs	N$_D$ = 1X10^{18}	
200 Å	AlGaAs	N$_D$ = 1X10^{18}	
50 Å	AlGaAs	NID	
5000 Å	GaAs	NID	
	GaAs	substrate	

FIG. 3. Structure of quasi-one-dimensional channel in the modulation-doped GaAs/Al$_{0.3}$Ga$_{0.7}$As.
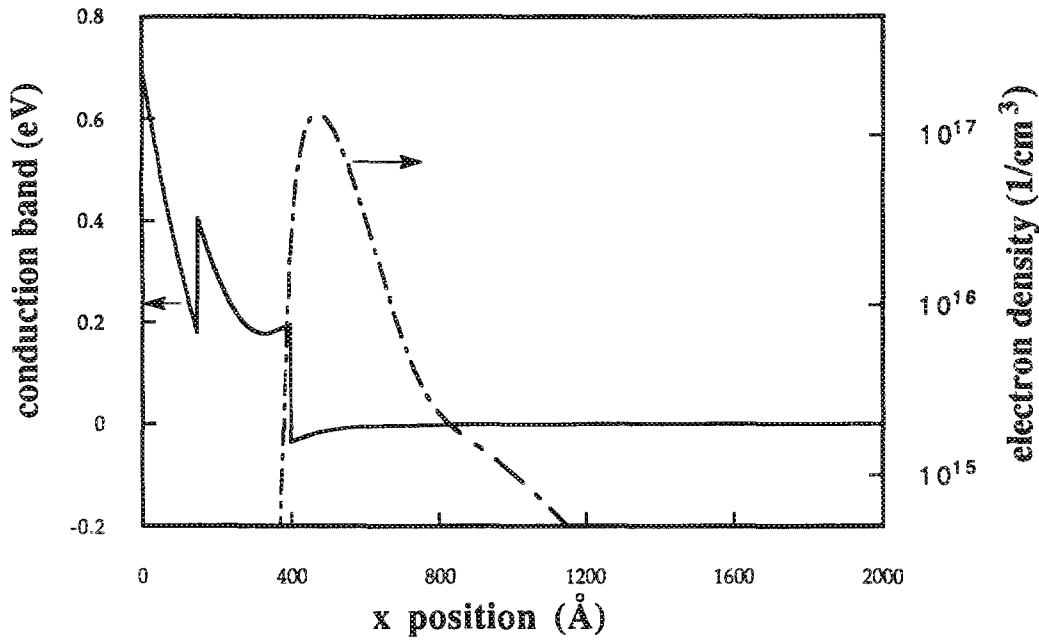
FIG. 4. Conduction band and the electron density distribution in the single-heterojunction GaAs/ $Al_{0.3}$ $Ga_{0.7}$As.

that allows use of nonuniform mesh size while preserving the symmetric property of the Schrödinger matrix equation. Newton's method is to solve the Poisson equation and find the modified conduction band. This method is especially suitable for finding the conduction band and the electron density distributed over large spatial dimensions, with higher computation efficiency and without loss of the accuracy.

Although we have only discussed the one-dimensional Schrödinger–Poisson solver, it is straightforward to extend this approach using a nonuniform mesh to the two-dimensional cases. We foresee that the computation efficiency of this method will be much higher than those using the conventional finite-difference or finite-element methods.

ACKNOWLEDGMENTS

APPENDIX: NEWTON'S METHOD IN SOLVING POISSON'S EQUATION

We show the generalization of Newton's method to solve Eq. (3). Since the electron density is determined by solutions of the Schrödinger equation which are in turn determined by the potential $\phi(x)$, the electron density is actually a functional of $\phi(x)$ via Eqs. (3), (4), and (5). Denoting this functional by $n[\phi]$, Poisson's equation (3) can be written as

$$\frac{d}{dx}\left(\epsilon_s \frac{d\phi}{dx}\right) = \frac{-q(N_D - n[\phi])}{\epsilon_0}. \tag{A1}$$

Let us denote the exact solution to Eq. (A1) by $\phi^{(0)}(x)$. For a given trial function $\phi(x)$, our task is to find the correction function $\delta\phi(x)$ so that

$$\phi^{(0)}(x) = \phi(x) + \delta\phi(x). \tag{A2}$$

Substituting (A2) into (A1), we obtain

$$\frac{d}{dx}\left(\epsilon_s \frac{d\phi}{dx}\right) = \frac{-q(N_D - n[\phi + \delta\phi])}{\epsilon_0} - \frac{d}{dx}\left(\epsilon_s \frac{d\delta\phi}{dx}\right). \tag{A3}$$

Defining

$$n[\phi + \delta\phi] = n[\phi] + \delta n[\phi], \tag{A4}$$

Eq. (A3) can be written as

$$-\left[\frac{d}{dx}\left(\epsilon_s \frac{d\phi}{dx}\right) + \frac{q}{\epsilon_0}(N_D - n[\phi])\right]$$
$$= \frac{d}{dx}\left(\epsilon_s \frac{d\delta\phi}{dx}\right) - \frac{q}{\epsilon_0}\delta n[\phi]. \tag{A5}$$

Note that the left-hand side of Eq. (A5) is the error in Poisson's equation for the trial function $\phi(x)$ which can be easily calculated. Assuming that $\delta\phi(x)$ is small, from Eqs. (5) and (A5), $\delta n[\phi]$ can be expressed as

$$\delta n[\phi] = \sum_{k=1}^{m} [\delta(\psi_k^*\psi_k)n_k + \psi_k^*\psi_k \delta n_k], \tag{A6}$$

where

$$\delta(\psi_k^*\psi_k) = \psi_k^*[\phi + \delta\phi]\psi_k[\phi + \delta\phi] - \psi_k^*[\phi]\psi_k[\phi] \tag{A7}$$

and

$$\delta n_k = n_k(\phi + \delta\phi) - n_k(\phi). \tag{A8}$$

Our numerical experience indicates that the first term on the right-hand side of Eq. (A6) is usually much smaller than the second one. Dropping the first term and expressing δn_k in terms of $\delta\phi$, explicitly, using Eqs. (4)–(6), we obtain

$$\delta n(\phi) = - \sum_{k=1}^{m} \psi_k \psi_k \frac{m^*}{\pi \hbar^2 (1 + e^{(E_k - E_F)/kT})}$$

$$\times \langle \psi_k | q \delta \phi | \psi_k \rangle, \tag{A9}$$

where $\langle | \rangle$ is the bra-ket integral.

Equations (A5)–(A9) are now the formula to solve for ϕ using the Newton method.

[1] T. Demel, D. Heitmann, P. Grambow, and K. Ploog, Appl. Phys. Lett. **53**, 2176 (1988).

[2] T. Thornton, M. Pepper, H. Ahmed, D. Andrews, and G. J. Davies, Phys. Rev. Lett. **56**, 1198 (1986).

[3] J. M. Gaines, P. M. Petroff, H. Kroemer, R. J. Simes, R. S. Geels, and J. H. English, J. Vac. Sci. Technol. B **6**, 1378 (1988).

[4] T. Fukui and H. Saito, Appl. Phys. Lett. **50**, 824 (1987).

[5] M. Tomizawa, T. Furuta, K. Yokoyama, and A. Yoshii, IEEE Trans. Electron Devices **ED-36**, 2380 (1989).

[6] D. Mui, M. Patil, and H. Morkoç, Appl. Phys. Lett. **55**, 1223 (1989).

[7] G. L. Snider, I-H. Tan, and E. L. Hu, J. Appl. Phys. **68**, 2849 (1990).

[8] S. E. Laux and F. Stern, Appl. Phys. Lett. **49**, 91 (1986).

[9] F. Szidarouszky and S. Yakowitz, *Principles and Procedures of Numerical Analysis* (Plenum, New York, 1978), p. 221.

[10] C. M. Krowne, J. Appl. Phys. **65**, 1602 (1989).

[11] J. Y.-F. Tang and S. E. Laux, IEEE Trans. Computer-Aided Design **CAD-5**, 645 (1986).

[12] F. B. Hildebrand, *Introduction to Numerical Analysis*, 2nd ed. (Dover, New York, 1987), p. 559.